A New Sulfur Oxide, OSOSO, and Its Cation, Likely Present in the Io's Atmosphere: Detection and Characterization by Mass Spectrometric and Theoretical Methods

Fulvio Cacace,[†] Romano Cipollini,[†] Giulia de Petris,*[,†] Marzio Rosi,[‡] and Anna Troiani[†]

Contribution from the Dipartimento di Studi di Chimica e Tecnologia delle Sostanze Biologicamente Attive, Università di Roma "La Sapienza", P. le Aldo Moro, 5-00185 Roma, Italy, and the Dipartimento di Chimica, Università di Perugia, Via Elce di Sotto, 8-06123 Perugia, Italy

Received July 12, 2000

Abstract: The gas-phase reaction of SO^+ with SO_2, relevant to the atmospheric chemistry of Io, was investigated with mass spectrometric and computational methods. Consistent with previous reports, no net chemical change was observed at $10^{-8}-10^{-7}$ Torr by FT-ICR spectrometry. However, formation of a transient $S_2O_3^+$ adduct of OSOSO connectivity, **a**, was suggested by the fast ($k = 6.0 \pm 1.5 \times 10^{-10}$ cm^{-3} s^{-1} molec^{-1}) $^{34}SO^+/^{32}SO_2$ isotope exchange. The adduct was directly observed in SO_2/CI experiments, and structurally probed by MIKE and CAD spectrometry, the results of which are also consistent with connectivity **a**. Computational results at the B3LYP/6-311+G(2d) level of theory, complemented by single-point CCSD(T) calculations, confirmed that a planar $S_2O_3^+$ ion of connectivity **a** is more stable at 298 K than the isomer **b** of connectivity $OSSO_2$ by 23.4 kcal mol^{-1} at the CCSD(T) level of theory. NR spectrometry of $S_2O_3^+$ allowed detection of a hitherto unknown sulfur oxide, S_2O_3, also of OSOSO connectivity, characterized as a metastable triplet whose dissociation into SO_2 and SO ($X^3\Sigma^-$), exothermic by 16.8 kcal mol^{-1} at 298 K, requires overcoming a barrier of 6.1 kcal mol^{-1} at the CCSD(T) level. The atmospheric implications of the results are briefly discussed.

Introduction

New impetus to the study of the gas-phase ion chemistry of sulfur oxides is provided by the results of the recent flyby of the orbiter Galileo to Io, the innermost moon of Jupiter. Its atmospheric gases, mostly SO_2 with 3−10 mol % SO, are found to escape from Io,[1] to be ionized by intense (10^9 w) electron beams,[2] forming a huge plasma cloud that contains, in addition to SO_2 and SO,[3] the corresponding molecular cations.[1,4] In short, Io's atmosphere can be regarded as a huge natural laboratory where gas-phase ion chemistry of sulfur oxides occurs on a large scale, for example the plasma cloud around Io is estimated to be depleted of ions by Jupiter's magnetosphere at the rate of some 10^3 kg s^{-1}, corresponding to a current of 2×10^9 A.[5]

Given its planetary relevance, we set out to investigate the gas-phase ion chemistry of sulfur oxides under conditions comparable to, and utilizing the same reagents present in, Io's atmosphere. The observational results leave no doubts as to the most relevant ion−molecule reaction, identifying as the neutral reagent, SO_2, by far the major atmospheric species, and as the charged reagent, SO^+, positively detected from its characteristic ion cyclotron waves.[4] The formation of the cation is traced to the dissociation of SO_2^+, formed in turn by electron impact ionization of the bulk neutral component,[6] another conceivable source being the exothermic charge exchange between SO_2^+ and SO, also a significant neutral component.[7]

On the basis of the above considerations, we have undertaken the study of the $SO^+ + SO_2$ reaction, focusing attention, in particular, on the detection and characterization of new species whose formation is peculiar to the unique natural environment represented by the atmosphere of Io. The results proved rewarding, because, in addition to the identification of the $S_2O_3^+$ cation of OSOSO connectivity, very likely present in Io's atmosphere, an unexpected bonus was the detection by neutralization−reionization (NR) mass spectrometry, and the theoretical characterization, of a new, simple sulfur oxide, S_2O_3, hitherto unknown and hence of considerable intrinsic interest.

Experimental Section

Materials. The gases were commercial research grade products with a stated purity exceeding 99.98 mol % and were used without further purification. The $S^{18}O_2$ sample was prepared by combustion of sulfur in $^{18}O_2$ (>99 mol ^{18}O% from Isotec, Inc.) at 400 °C, 400 Torr and was purified according to standard vacuum procedures.

Instruments. The FT-ICR experiments were performed with a model 47e APEX spectrometer (Bruker Spectrospin) equipped with an external EI/CI ion source, and a cylindrical "infinity" cell,[8] in addition to a pulsed valve and a Bayard-Alpert ionization gauge, whose readings were corrected according to standard procedures.[9] The MIKE and CAD spectra, as well as the NR spectra, were recorded utilizing a version of the ZAB Spec oa-TOF instrument (Micromass Ltd.) whose design was previously illustrated.[10] Briefly, the ions from the EI/CI source enter the first electrostatic sector, are mass-selected by the magnet, and enter

[†] "La Sapienza" University of Rome.

[‡] Perugia University.

(1) Russel, C. T.; Kivelson, M. G. *Science* **2000**, *287*, 1998.

(2) Williams, D. J. Project Galileo Homepage, http:/www.jpl.nasa.gov//galileo/status961023.html.

(3) Lellouch, E. *Icarus* **1996**, *124*, 1 and references therein.

(4) Küppers, M.; Schneider, N. M. *Geophys. Res. Lett.* **2000**, *27*, 513.

(5) Galileo project: Galileo Moons: Io. http://galileo.jpl.nasa.gov/moons/io.html.

(6) Decker, D. K.; Adams, N. G.; Babcock, L. M. *Int. J. Mass Spectrom.* **2000**, *195−196*, 185.

(7) The IP of SO and SO_2 are 10.32 and 12.32 eV, respectively, Lias, S. G.; Bartmess, J. E.; Liebman, T. F.; Holmes, J. L.; Levin, R. D.; Mallard, W. G. *J. Phys. Chem. Ref. Data* **1988**, *17*, suppl. 1.

(8) Caravatti, P.; Allemann, M. *Org. Mass Spectrom.* **1991**, *26*, 514.

(9) Bartmess, J. E.; Georgiadis, R. M. *Vacuum* **1983**, *33*, 149.

10.1021/ja002533d CCC: $20.00
Published on Web 12/29/2000

the first pair of collision cells, to which different gases can be admitted through individual valves. Any desired voltage of the cells with respect to ground can be selected, and if desired, charged species from the first cell can be prevented from entering the second one by a deflecting electrode. Next, the ions are analyzed in the second electrostatic sector and enter the second pair of gas collision cells before reaching the detector. When required, application of a proper potential to a steering electrode ("pusher") allows introducing the ions into the orthogonal TOF spectrometer, equipped with a microchannel plate (MCP) detector.

Procedure. The ions from the external source were transferred into the FT-ICR cell containing the neutral reagent at a stationary pressure of $10^{-8}-10^{-7}$ Torr. The ions were isolated by a broad-band ("chirp") ejection, followed by single-frequency pulse ("single shots"). Thermalization of the ions was achieved by allowing a suitable "cooling" (1 s) time before recording their reaction kinetics, or by collision with Ar, temporarily admitted into the cell through the pulsed valve.[11] The pseudo-first-order rate constant was obtained from the slope of the logarithmic plot of the relative ion intensity versus the reaction time. The number density of the neutral molecules was calculated from the pressure readings of the Bayard-Alpert gauge, corrected according to a standard procedure based on the correlation between relative sensitivity and the polarizability of the gas,[9] and calibrated utilizing as a standard the known rate constant for the $CH_4^+ + CH_4 \rightarrow CH_5^+ + CH_3$ process.[12] The efficiency of the reaction was expressed as the ratio of its bimolecular rate constant to the collision rate constant calculated according to the ADO theory, or by the Su and Chesnavich parametrized variational theory,[13] that gave closely similar results.

MIKE, CAD, and NR Spectrometry. The ions were generated in the CI source of the ZAB Spec oa-TOF instrument from SO_2 (0.1 Torr, 393 K), under the following conditions: accelerating voltage 8 keV (4 keV in NR experiments), emission current 0.5 mA, repeller voltage 0 V. In the CAD experiments He was introduced into the first collision cell to such pressure as to reduce the intensity of the beam to ~30%. The NR experiments were performed in the first pair of collision cells located between the magnet and the second electrostatic sector, using Xe as the neutralizing collider at a pressure adjusted to achieve an 80% transmittance. Reionization was performed using O_2 as the collider, at approximately the same transmittance. Any ions surviving neutralization were deflected away from the beam using a high-voltage (1 keV) electrode, whose efficiency was checked by control experiments. Each NR spectrum is the average of 30−50 acquisitions to improve the signal-to-noise ratio.

Computational Details. Density functional theory, using the hybrid[14] B3LYP functional,[15] was used to localize the stationary points of the investigated systems and to evaluate the vibrational frequencies. Although it is well-known that density functional methods using the nonhybrid functional sometimes tend to overestimate bond lengths, using the B3LYP hybrid functional usually provides geometrical parameters in excellent agreement with experiment.[16] Single-point energy calculations at the optimized geometries were performed using the coupled-cluster single- and double-excitation method[17] with a pertubational estimate of the triple-excitation (CCSD(T) approach[17]) to include extensively correlation contributions.[18] Transition states were located using the synchronous transit-guided quasi-Newton method from Schlegel and co-workers.[19] The 6-311+G(2d) basis set was used for both the B3LYP and the CCSD(T) calculations.[20] Zero-point energy corrections evaluated at B3LYP/6-311+G(2d) level were added to the CCSD(T) energies. The 0 K total energies of the species of interest were corrected to 298 K by adding translation, rotational, and vibrational contributions. The absolute entropies were calculated by using standard statistical-mechanistic procedure from scaled harmonic frequencies and moments of inertia relative to B3LYP/6-311+G(2d) optimized geometries. All calculations were performed using Gaussian 98[21] on an SGI Origin 2000 computer and on a cluster of IBM RISC/6000 workstations.

Results

According to the available literature data[12] SO^+ is unreactive toward SO_2, which would deny the very occurrence of the reaction that appears most relevant to the ion chemistry in the Io's atmosphere. To clarify the issue, we reexamined the reaction by FT-ICR and CI mass spectrometry.

FT-ICR Evidence. Experiments performed at 298 K at pressures of the order of 10^{-8} Torr confirmed that no net chemical change takes place upon reaction of thermalized SO^+ ions with SO_2. Nevertheless, when the $^{34}S^{16}O^+$ isotopomer was allowed to react with sulfur dioxide of natural isotopic composition, the isotope exchange

$$^{34}S^{16}O^+ + {}^{32}S^{16}O_2 \rightarrow {}^{32}S^{16}O^+ (+ {}^{34}S^{16}O_2) \qquad (1)$$

was observed and positively demonstrated by accurate mass measurements. Reaction 1 is fast, $k_1 = 6.0 \pm 1.5 \times 10^{-10}$ cm^3 s^{-1} molec^{-1} which, considering the isotopic composition of natural SO_2 and the intrinsic 50% efficiency limit of the isotopic exchange, corresponds to a collisional efficiency, k_1/k_{coll}, of ~40%. The occurrence of exchange 1 points to the transient formation of an ion−molecule adduct, that cannot be collisionally stabilized and hence cannot be detected, in the low-pressure range of FT-ICR experiments. Not only do the FT-ICR results show promise of a successful stabilization of the SO^+SO_2 adduct at higher pressures, but the remarkable efficiency of the isotope exchange 1 is also structurally informative. Indeed, it suggests that the transient complex contains two preformed, equivalent, and easily exchangeable units, which would be consistent with the connectivity **a**.

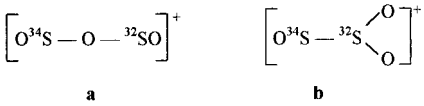

a **b**

Conversely, isotope exchange within a complex of connectivity **b** would involve an energetically and entropically demanding mechanism, requiring fission of a strong S=O double bond,

(10) Bernardi, F.; Cacace, F.; de Petris, G.; Pepi, F.; Rossi, I.; Troiani, A. *Chem. Eur. J.* **2000**, *6*, 537.
(11) Nixdorf, A.; Grützmacher, H.-F. *Eur. Mass Spectrom.* **1999**, *5*, 93.
(12) Anicich, V. G. *J. Phys. Chem. Ref. Data* **1993**, *22*, 1469.
(13) (a) Bowers, M. T.; Su, T. *Interactions between Ions and Molecules*; Plenum Press: New York, 1975; p 163. (b) Su, T.; Chesnavich, J. *J. Chem. Phys.* **1982**, *76*, 5183.
(14) Becke, A. D. *J. Chem. Phys.* **1993**, *98*, 5648.
(15) Stevens, P. J.; Devlin, F. J.; Chablowshi, C. F.; Frisch, M. J. *J. Phys. Chem.* **1994**, *98*, 11623.
(16) Bauschlicher, C. W.; Ricca, A.; Partridge, H.; Langhoff, S. R. In *Recent Advances in Density Functional Theory*; Chong, D. P., Ed.; World Scientific Publishing Co.; Singapore, 1997; Part II.
(17) Bartlett, R. J. *Annu. Rev. Phys. Chem.* **1981**, *32*, 359.
(18) Olsen, J.; Jorgensen, P.; Koch, H.; Balkova, A.; Bartlett, R. J. *J. Chem. Phys.* **1996**, *104*, 8007.
(19) (a) Peng, C.; Schlegel, H. B. *Isr. J. Chem.* **1993**, *33*, 449. (b) Peng, C.; Ayala, P. Y.; Schlegel, H. B.; Frisch, M. J. *J. Comput. Chem.* **1996**, *17*, 49.
(20) (a) Krishnam R.; Binkley, J. S.; Seeger, R.; Pople, J. A. *J. Chem. Phys.* **1980**, *72*, 650. (b) McLean, A. D.; Chandler, G. S. *J. Chem. Phys.* **1980**, *72*, 5639. (c) Clark, T.; Chandrasekhar, J.; Spitznagel, G. W.; Schleyer, P.v. R. *J. Comput. Chem.* **1983**, *4*, 294. (d) Frisch, M. J.; Pople, J. A.; Binkley, J. S. *J. Chem. Phys.* **1984**, *80*, 3265. (e) Raghavachari, K.; Trucks, G. W.; Pople, J. A.; Head-Gordon, M. *Chem. Phys. Lett.* **1989**, *157*, 479.
(21) Frisch, M. J.; Trucks, G. W.; Schlegel, H. B.; Scuseria, G. E.; Robb, M. A.; Cheeseman, Zakrzewski, V. G.; Montgomery, J. A., Jr.; Stratmann, R. E.; Burant, J. C.; Dapprich, S.; Millam, J. M.; Daniels, A. D.; Kudin, K. N.; Strain, M. C.; Farkas, O.; Tomasi, J.; Barone, V.; Cossi, M.; Cammi, R.; Mennucci, B.; Pomelli, C.; Adamo, C.; Clifford, S.; Ochterski, J.; Petersson, G. A.; Ayala, P. Y.; Cui, Q.; Morokuma, K.; Malick, D. K.; Rabuck, A. D.; Raghavachari, K.; Foresman, J. B.; Cioslowski, J.; Ortiz, J. V.; Baboul, A. G.; Stefanov, B. B.; Liu, G.; Liashenko, A.; Piskorz, P.; Komaromi, I.; Gomperts, R.; Martin, R. L.; Fox, D. J.; Keith, T.; Al-Laham, M. A.; Peng, C. Y.; Nanayakkara, A.; Gonzalez, C.; Challacombe, M.; Gill, P. M. W.; Johnson, B.; Chen, W.; Wong, M. W.; Andres, J. L.; Gonzalez, C.; Head-Gordon, M.; Replogle, E. S.; Pople, J. A. *Gaussian 98*, rev. A.7; Gaussian, Inc.: Pittsburgh, PA, 1998.

Table 1. Collisionally Activated Dissociation (CAD) Spectra of Different $S_2O_3^+$ Isotopomers

$^{32}S_2{}^{16}O_3^+$		$^{34}S^{32}S^{16}O_3^+$		$^{32}S_2{}^{18}O_3^+$		$^{34}S^{32}S^{18}O_3^+$		assignments[a]	
m/z	*I* (%Σ)[b]	*m/z*	*I* (%Σ)[b]	*m/z*	*I* (%Σ)[b]	*m/z*	*I* (%Σ)[b]		
96	2.0	98	2.1	100	1.6	102	1.8	$S_2O_2^+$	[$^{32}S_2{}^{16}O_2^+$, $^{34}S^{32}S^{16}O_2^+$, $^{32}S_2{}^{18}O_2^+$, $^{34}S^{32}S^{18}O_2^+$]
80	0.3	82	0.5	82	0.3	84	0.3	S_2O^+	[$^{32}S_2{}^{16}O^+$, $^{34}S^{32}S^{16}O^+$, $^{32}S_2{}^{18}O^+$, $^{34}S^{32}S^{18}O^+$]
64	33.8	66	17.5	68	35.7	70	18.7	SO_2^+[c]	[$^{32}S^{16}O_2^+$, $^{34}S^{16}O_2^+$, $^{32}S^{18}O_2^+$, $^{34}S^{18}O_2^+$]
		64	15.0			68	17.1	SO_2^+[c]	[$^{32}S^{16}O_2^+$, $^{32}S^{18}O_2^+$]
48	62.2	50	31.7	50	60.9	52	30.3	SO^+[c]	[$^{32}S^{16}O^+$, $^{34}S^{16}O^+$, $^{32}S^{18}O^+$, $^{34}S^{18}O^+$]
		48	31.5			50	30.0	SO^+[c]	[$^{32}S^{16}O+$, $^{32}S^{18}O^+$]
32	1.7	34	0.8	32	1.5	34	0.9	S+	[$^{32}S^+$, $^{34}S^+$]
		32	0.9			32	0.9	S^+	[$^{32}S^+$]

[a] In parentheses the isotopomers of the CAD fragments. [b] Percentage of the fragments intensity with respect to the total fragments intensities, standard deviation ±10%. [c] These fragments are also present in the MIKE spectra.

hardly competitive with the facile back dissociation of **b** into its monomers, $^{34}SO^+$ and $^{32}SO_2$. In summary, the evidence from the FT-ICR experiments suggests that the alleged lack of reactivity of SO^+ toward SO_2 may simply reflect the dissociation of the reaction product in low-pressure experiments and that the product would have connectivity **a**, without any S−S bond.

CI Experiments. Formation of $S_2O_3^+$, inferred from the low-pressure FT-ICR spectrometry, was directly observed in CI experiments, performed at higher pressures that allow collisional stabilization of the adduct

$$SO^+ + SO_2 \rightleftarrows [S_2O_3]^+_{exc} \xrightarrow{+M,\ -M^*} S_2O_3{}^+ \qquad (2)$$

The CI spectra recorded in neat SO_2 at 393 K, ∼0.1 Torr, display the following major ions (in parentheses the relative intensities): SO_2^+ (100), SO^+ (62), $(SO_2)_2^+$ (19), S^+ (17), $S_2O_3^+$ (11).

The structure of the $S_2O_3^+$ ions was probed by MIKE and CAD spectrometry, the results of which are reported in Table 1. Given the low mass resolution achievable in these experiments, the necessary discrimination between ions containing one ^{32}S atom and those containing two ^{16}O atoms could not be obtained by accurate mass analysis, as is feasible in FT-ICR spectrometry. The problem was tackled by comparing the MIKE and CAD spectra of the $^{32}S_2{}^{16}O_3^+$ and $^{32}S^{34}S^{16}O_3^+$ ions from SO_2 of natural composition and also of the $^{32}S_2{}^{18}O_3^+$ and $^{32}S^{34}S^{18}O_3^+$ ions from ^{18}O-labeled SO_2 (Table 1). Further support was obtained from the MS^3 spectra of the fragments from the above ions. The results allow one to assign the two weak metastable peaks observed to SO^+ and SO_2^+, present also in the CAD spectra together with purely collisional S^+, S_2O^+, and $S_2O_2^+$ fragments. All fragmentation processes observed are consistent with the assignment of connectivity **a** to the ion probed, in that they arise from the fission of one or two bonds of the parent species. However, although unlikely, the presence of ions of connectivity **b**, or of a mixed **a/b** population, cannot be excluded by MIKE and CAD spectrometry alone.

NR Experiments. The $^+NR^+$ spectra, illustrated in Figure 1, display significant "recovery"peaks, showing that neutral S_2O_3 exists as an isolated species in the gas phase, with a lifetime in excess of 1 μs.

Computational Results. The optimized geometries of the minima localized at B3LYP level on the potential energy surface of $[S_2O_3]^+$ are shown in Figure 2 and Table 2, that gives as well their total energies and frequencies. The lowest minimum (**A**) is a planar species which can be seen as an electrostatic complex between SO_2 and SO^+, with connectivity OSOSO. This species is stable with respect to dissociation into SO_2 and SO^+ by 32.2 kcal mol^{-1} at B3LYP level and by 25.3 kcal mol^{-1} at CCSD(T) level at 298 K. At higher energy we have species **B** which is planar, and it is bound by 10.6 kcal mol^{-1} at B3LYP level and by 1.9 kcal mol^{-1} at CCSD(T) level at 298 K. This

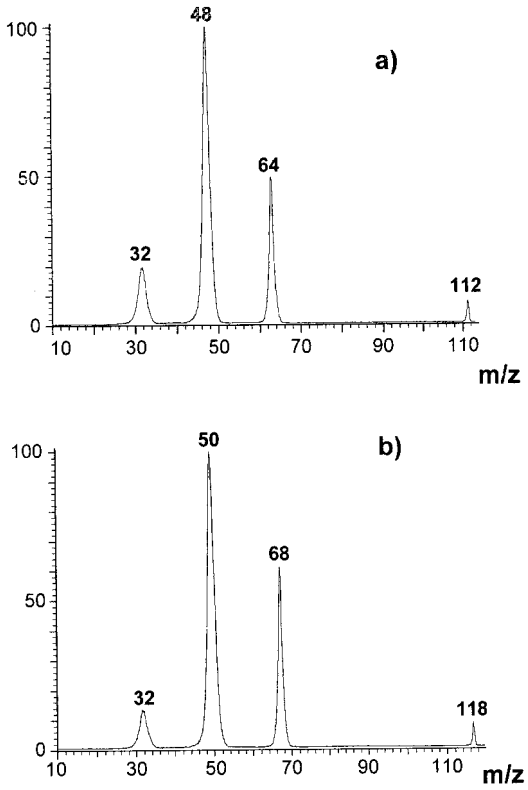

Figure 1. $^+NR^+$ spectra of (a) the $^{32}S_2{}^{16}O_3^+$ ion, (b) the $^{32}S_2{}^{18}O_3^+$ ion. Note the "recovery" peaks at the *m/z* ratios of the parent cations.

species shows $OSSO_2$ connectivity. At even higher energy we can find species **C** and **D**, which both show C_s symmetry and are unstable with respect to dissociation. Figure 3 shows the structures of the minima localized on the triplet surface of neutral S_2O_3, whereas Figure 4 illustrates the minima of the singlet surface. Optimized geometries, total energies, and frequencies for the triplet and singlet states are reported in Tables 3 and 4, respectively. The lowest triplet ($\mathbf{T_1}$) is unstable with respect to dissociation into SO_2 and SO ($X^3\Sigma^-$) by 10.2 kcal mol^{-1} at B3LYP level and 16.8 kcal mol^{-1} at CCSD(T) level at 298 K. However, the dissociation of $\mathbf{T_1}$ into SO_2 and SO ($X^3\Sigma^-$) at 298 K shows a barrier of 3.8 kcal mol^{-1} at B3LYP level and 6.1 kcal mol^{-1} at CCSD(T) level. The geometry of the transition state at the saddle point is also illustrated in Figure 3. We could not find a triplet with the same structure of cation **B**, suggesting that this neutral species should be unbound also at B3LYP level.

The lowest singlet is the planar species **S1**, which is unstable with respect to dissociation into SO_2 and SO ($X^3\Sigma^-$) by 19.2 kcal mol^{-1} at B3LYP level and by 21.5 kcal mol^{-1} at CCSD(T) level at 298 K. However, this is a spin-forbidden reaction. The first excited singlet state of SO is $a^1\Delta$. The dissociation of $\mathbf{S_1}$ into SO_2 and SO ($a^1\Delta$) is endothermic by 9.12 kcal mol^{-1} at

Table 2. Total energies, Geometries, and Vibrational Frequencies (Intensities) of the $S_2O_3^+$ Species[a]

	A $^2A''$		**B** $^2A''$		**C** $^2A''$		**D** $^2A''$
E_{B3LYP}	−1021.774411		−1021.741412		−1021.681666		−1021.590624
ZPE[b]	0.011087		0.011472		0.013046		0.012378
$E_{CCSD(T)}$	−1020.300103		−1020.263188		−1020.207421		−1020.118851
a″	29.6 (1.8)	a″	61.2 (7.7)	a″	205.9 (0.3)	a′	246.0 (0.8)
a′	79.1 (1.8)	a′	77.4 (2.3)	a′	275.3 (6.3)	a″	282.8 (2.7)
a″	171.6 (18.6)	a′	124.9 (21.3)	a′	370.2 (25.5)	a′	357.2 (16.1)
a′	215.6 (6.6)	a″	170.6 (9.9)	a″	382.6 (12.5)	a″	368.6 (10.0)
a′	293.4 (95.6)	a′	248.1 (23.8)	a′	443.1 (18.7)	a′	483.0 (26.8)
a′	527.5 (19.7)	a′	497.3 (35.1)	a′	621.4 (120.5)	a′	600.9 (28.7)
a′	976.0 (299.0)	a′	1163.1 (46.0)	a′	793.4 (30.7)	a″	735.5 (5.7)
a′	1277.6 (72.2)	a′	1263.7 (72.8)	a′	1186.3 (114.9)	a′	981.2 (36.4)
a′	1323.6 (132.0)	a′	1429.4 (106.6)	a″	1448.3 (96.6)	a′	1378.1 (83.9)
$r(S_2O_1)$	1.427	$r(S_2O_1)$	1.428	$r(S_2O_1)$	1.709	$r(S_2O_1)$	1.413
$r(O_3S_2)$	1.508	$r(O_3S_2)$	1.428	$r(S_3S_2)$	2.188	$r(S_3S_2)$	2.051
$\angle(O_3S_2O_1)$	116.9	$\angle(O_3S_2O_1)$	127.7	$\angle(S_3S_2O_1)$	48.8	$\angle(S_3S_2O_1)$	119.8
$r(S_4O_3)$	2.074	$r(S_4S_2)$	2.624	$r(O_4S_3)$	1.418	$r(O_4S_2)$	1.593
$\angle(S_4O_3S_2)$	137.6	$\angle(S_4S_2O_3)$	114.5	$\angle(O_4S_3S_2)$	113.1	$\angle(O_4S_2S_3)$	110.0
$\angle(S_4O_3S_2O_1)$	0.0	$\angle(S_4S_2O_3O_1)$	180.0	$\angle(O_4S_3S_2O_1)$	−99.9	$\angle(O_4S_2S_3O_1)$	148.3
$r(O_5S_4)$	1.441	$r(O_5S_4)$	1.445	$r(O_5S_3)$	1.418	$r(O_5O_4)$	1.573
$\angle(O_5S_4O_3)$	112.1	$\angle(O_5S_4S_2)$	105.7	$\angle(O_5S_3S_2)$	113.1	$\angle(O_5O_4S_2)$	60.4
$\angle(O_5S_4O_3S_2)$	0.0	$\angle(O_5S_4S_2O_1)$	180.0	$\angle(O_5S_3S_2O_1)$	99.9	$\angle(O_5O_4S_2O_1)$	−110.4

[a] Total energies in hartrees, bond lengths in Å, angles in degrees, frequencies in cm^{-1}, intensities in km/mol. [b] Zero-point energy.

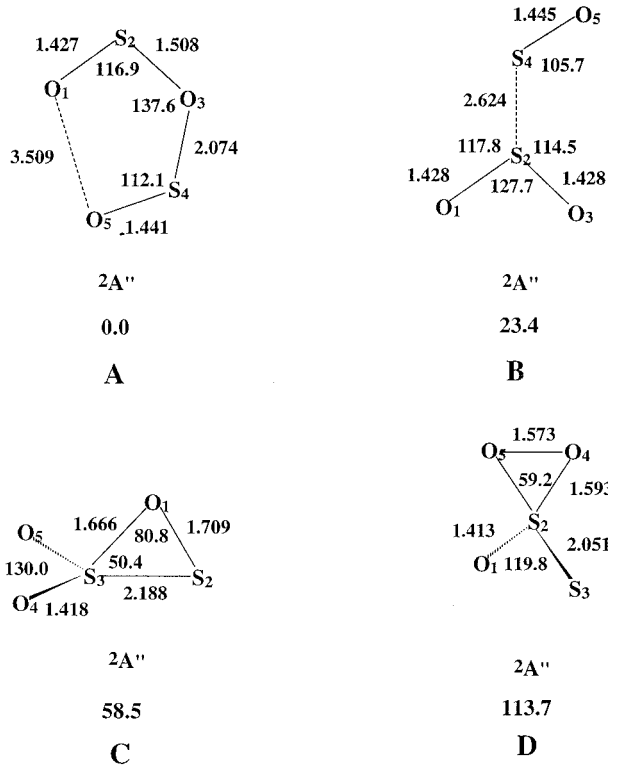

Figure 2. Selected geometrical parameters (in Å and degrees) and CCDS(T) relative energies at 298 K of relevant minima on the $S_2O_3^+$ surface.

Figure 3. Selected geometrical parameters (in Å and degrees) and CCSD(T) relative energies at 298 K of relevant minima and TS on the S_2O_3 triplet surface.

B3LYP and only by 2.3 kcal mol^{-1} at CCSD(T) level of calculation at 298 K. The localization of species **S_2** on the singlet surface should be ascribed only to the overestimation of the singlet−triplet splitting of SO at the B3LYP level of computation. Indeed, species **S_2** is computed to be stable with respect to dissociation into singlet fragments at 298 K by 8 kcal mol^{-1} at B3LYP level, but it is unstable by 2.4 kcal mol^{-1} at CCSD(T) level. Species **S_3** and **S_4** lie at higher energy and both show C_s symmetry. By combining the computational results with the known heats of formation of SO^+, SO, and SO_2[7] one can estimate the formation enthalpies of $S_2O_3^+$ and S_2O_3, 143.0 and −52.9 kcal mol^{-1}, respectively, referred to cation **A** and triplet **T1**. Furthermore, one can roughly estimate the IP of the S_2O_3 triplet **T1**, namely ∼8.5 eV, to be compared with the 10.3 eV IP of free SO.[7] Visual inspection of the above energetic features is allowed by the energy diagram illustrated in Figure 5.

Discussion

The $S_2O_3^+$ Cation. The evidence from FT-ICR mass spectrometry, in particular the high efficiency of the isotope exchange 1, strongly suggests the transient formation of a

Table 3. Total Energies, Geometries, and Vibrational Frequencies (Intensities) of the Triplet S_2O_3 Species[a]

	$\mathbf{T_1}$ ^3B		$\mathbf{T_2}$ $^3A_1$		$\mathbf{TS(T_1 \rightarrow SO_2 + SO)}$ ^3A
E_{B3LYP}	−1022.094882		−1022.043984		−1022.087736
ZPE[b]	0.010252		0.012071		0.009509
$E_{CCSD(T)}$	−1020.601795		−1020.566636		−1020.591053
a	41.9 (5.9)	a_l	72.4 (17.9)	a	441.5*i*
b	81.6 (8.0)	e	91.6 (0.1)	a	72.7
a	160.5 (2.1)	a_1	466.4 (163.0)	a	105.7
b	387.2 (17.5)	e	490.7 (23.7)	a	135.4
a	414.0 (0.4)	a_l	1021.2 (17.2)	a	356.3
b	564.7 (401.3)	e	1287.0 (193.5)	a	461.2
a	566.2 (30.7)			a	730.0
b	1134.7 (130.3)			a	1144.0
a	1149.3 (35.8)			a	1168.8
$r(S_2O_1)$	1.477	$r(S_2S_1)$	2.459	$r(S_2O_1)$	1.472
$r(O_3S_2)$	1.706	$r(O_3S_2)$	1.443	$r(O_3S_2)$	1.561
$\angle(O_3S_2O_1)$	109.7	$\angle(O_3S_2S_1)$	96.1	$\angle(O_3S_2O_1)$	112.8
$r(S_4O_3)$	1.706	$r(O_4S_2)$	1.443	$r(S_4O_3)$	2.038
$\angle(S_4O_3S_2)$	120.9	$\angle(O_4S_2S_1)$	96.1	$\angle(S_4O_3S_2)$	117.9
$\angle(S_4O_3S_2O_1)$	64.7	$(O_4S_2S_1O_3)$	−120.0	$\angle(S_4O_3S_2O_1)$	82.8
$r(O_5S_4)$	1.477	$r(O_5S_2)$	1.443	$r(O_5S_4)$	1.476
$\angle(O_5S_4O_3)$	109.7	$\angle(O_5S_2S_1)$	96.1	$\angle(O_5S_4O_3)$	105.9
$\angle(O_5S_4O_3S_2)$	64.7	$\angle(O_5S_2S_1O_3)$	120.0	$(O_5S_4O_3S_2)$	15.4

[a] Total energies in hartrees, bond lengths in Å, angles in degrees, frequencies in cm^{-1}, intensities in km/mol. [b] Zero-point energy.

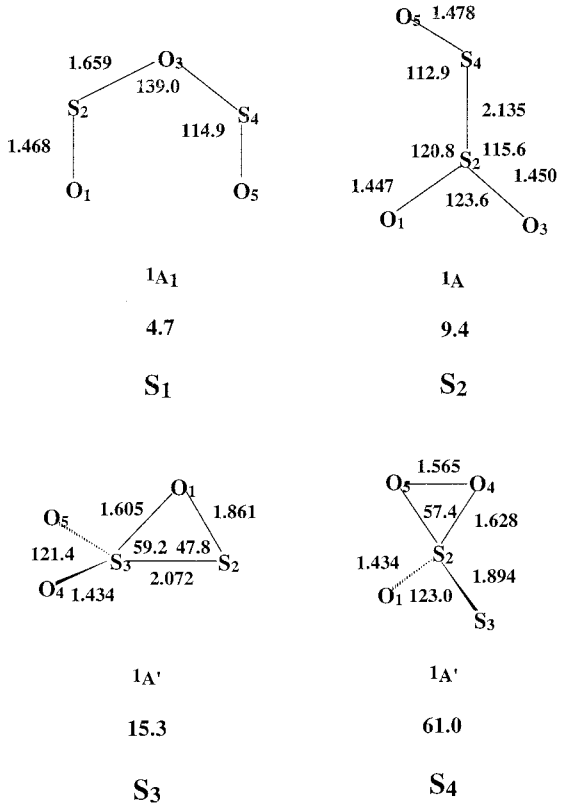

Figure 4. Selected geometrical parameters (in Å and degrees) and CCSD(T) relative energies at 298 K of relevant minima on the S_2O_3 singlet surface.

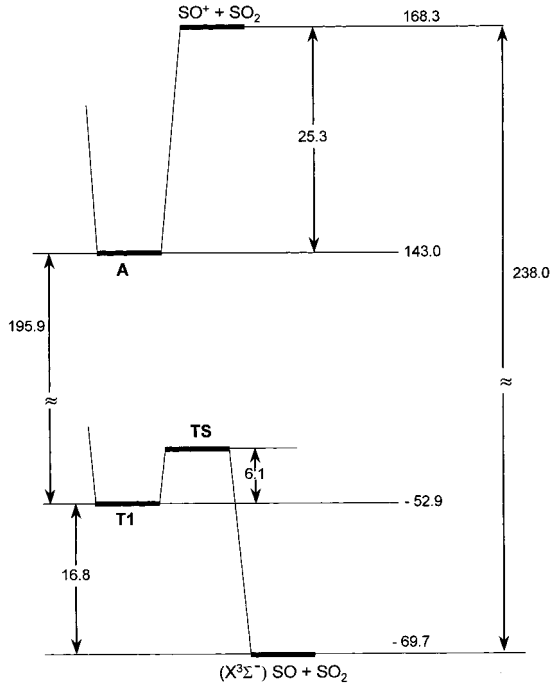

Figure 5. Simplified energy diagram showing the formation enthalpies (kcal mol^{-1}) of the most stable $S_2O_3^+$ and S_2O_3 species (see text).

charged complex of OSOSO connectivity that however contains enough internal energy to undergo back dissociation in the lack of radiative or collisional stabilization, and hence cannot be detected in FT-ICR experiments. The higher-pressure range typical of CI experiments allows partial stabilization of the adduct, whose OSOSO connectivity is consistent with the MIKE and CAD evidence. The experimental assignment is supported by the theoretical results, showing that at 298 K the stability of species **A** of connectivity **a** exceeds that of the isomer **B** of connectivity **b** by 21.6 kcal mol^{-1} at the B3LYP level and 23.4 kcal mol^{-1} at the CCSD(T) level. Such a large stability difference suggests that the $S_2O_3^+$ population probed by MIKE and CAD spectrometry consists of ions **a**. Although formation of ions **b** is also energetically allowed, and might be kinetically favored, any ions **b** initially formed would be converted into isomer **a** before leaving the CI source by collision with the molecules of the bulk gas, according to the reaction

$$\underset{\mathbf{b}}{[OS\ SO_2]^+} + SO_2 \rightarrow \underset{\mathbf{a}}{[OSOSO]^+} + SO_2 \qquad (3)$$

presumably very fast, being in essence a strongly exothermic ligand exchange undergone by an electrostatically bound complex. In summary, the present study shows that SO^+ in *not* unreactive toward SO_2, undergoing instead an exothermic

Table 4. Total Energies, Geometries, and Vibrational Frequencies (Intensities) of the Singlet S_2O_3 Species[a]

		$\mathbf{S_1}$ $^1A_1$		$\mathbf{S_2}$ ^1A		$\mathbf{S_3}$ $^1A'$		$\mathbf{S_4}$ $^1A'$
E_{B3LYP}		−1022.080576		−1022.079697		−1022.060488		−1021.987925
ZPE[b]		0.010518		0.011731		0.013471		0.012565
$E_{CCSD(T)}$		−1020.594411		−1020.588034		−1020.579214		−1020.505604
	a_2	101.4 (0)	a	130.4 (5.2)	a″	230.7 (0.2)	a″	249.5 (0)
	a_1	115.8 (0.1)	a	134.9 (7.7)	a′	360.5 (1.6)	a′	307.4 (1.2)
	b_2	267.6 (17.4)	a	186.6 (1.6)	a″	412.1 (11.6)	a″	397.2 (7.1)
	b_l	269.0 (20.8)	a	229.0 (3.4)	a′	458.7 (12.8)	a′	422.2 (19.8)
	b_2	457.2 (25.4)	a	372.8 (9.3)	a′	509.8 (12.2)	a′	566.3 (14.6)
	a_1	510.7 (21.9)	a	515.0 (27.4)	a′	604.0 (132.6)	a″	609.7 (13.5)
	a_l	536.1 (3.3)	a	1094.5 (349.6)	a′	794.6 (40.6)	a′	723.9 (159.9)
	b_2	1156.3 (314.5)	a	1153.4 (59.0)	a′	1182.9 (225.6)	a′	956.4 (150.2)
	a_l	1202.6 (152.7)	a	1332.7 (166.9)	a″	1359.5 (185.7)	a′	1282.6 (184.2)
	$r(S_2O_1)$	1.468	$r(S_2O_1)$	1.447	$r(S_2O_1)$	1.861	$r(S_2O_1)$	1.434
	$r(O_3S_2)$	1.659	$r(O_3S_2)$	1.450	$r(S_3S_2)$	2.072	$r(S_3S_2)$	1.894
	$\angle(O_3S_2O_1)$	114.9	$\angle(O_3S_2O_1)$	123.6	$\angle(S_3S_2O_1)$	47.8	$\angle(S_3S_2O_1)$	123.0
	$r(S_4O_3)$	1.659	$r(S_4S_2)$	2.135	$r(O_4S_3)$	1.434	$r(O_4S_2)$	1.628
	$\angle(S_4O_3S_2)$	139.0	$\angle(S_4S_2O_3)$	115.6	$\angle(O_4S_3S_2)$	116.7	$\angle(O_4S_2S_3)$	116.2
	$\angle(S_4O_3S_2O_1)$	0.0	$\angle(S_4S_2O_3O_1)$	180.0	$\angle(S_4S_3S_2O_1)$	−102.6	$\angle(O_4S_2S_3O_1)$	−147.6
	$r(O_5S_4)$	1.468	$r(O_5S_4)$	1.478	$r(O_5S_3)$	1.434	$r(O_5O_4)$	1.565
	$\angle(O_5S_4O_3)$	114.9	$\angle(O_5S_4S_2)$	112.9	$\angle(O_5S_3S_2)$	116.7	$\angle(O_5O_4S_2)$	61.3
	$\angle(O_5S_4O_3S_2)$	0.0	$\angle(O_5S_4S_2O_1)$	0.0	$\angle(O_5S_3S_2O_1)$	102.6	$\angle(O_5O_4S_2O_1)$	103.6

[a] Total energies in hartrees, bond lengths in Å, angles in degrees, frequencies in cm^{-1}, intensities in km/mol. [b] Zero-point energy.

addition whose product, $S_2O_3^+$, is characterized by the OSOSO connectivity deduced from the mutually supporting experimental and theoretical evidence. As to the nature of the OS−OSO bond, its dissociation energy, as high as 25 kcal mol^{-1}, exceeds that typical of a purely electrostatic interaction and suggests a significant covalent character. This is not the case of the OS−SO_2 bond in isomer **b**, whose dissociation energy, computed to be <10.6 kcal mol^{-1}, is typical of a purely electrostatic interaction.

The New Sulfur Oxide, S_2O_3. Given the vertical character of the neutralization process,[22] the S_2O_3 species detected by NR spectrometry must be assigned the OSOSO connectivity of the parent cation. Indeed, species $\mathbf{T_1}$ of this connectivity is theoretically characterized as the most stable minimum on the S_2O_3 triplet surface. Whereas at the CCSD(T) level $\mathbf{T_1}$ is unstable with respect to dissociation into SO_2 and SO ($X^3\Sigma^-$) by 16.8 kcal mol^{-1} at 298 K, the process requires overcoming a barrier of 6.1 kcal mol^{-1}. We were unable to find a triplet with the $OSSO_2$ connectivity of cation **B**, which suggests that the corresponding neutral is unbound. The lowest minimum on the S_2O_3 singlet surface, the planar species $\mathbf{S_1}$, is unstable with respect to the spin-forbidden dissociation into SO_2 and SO ($X^3\Sigma^-$) by 21.5 kcal mol^{-1} at 298 K at the CCSD(T) level of theory. Spin-allowed dissociation of $\mathbf{S_1}$ into SO_2 and SO ($a^1\Delta$), the first excited singlet of SO, is computed to be endothermic by only 2.3 kcal mol^{-1} at 298 K at the CCSD(T) level. Nevertheless, the theoretical approach utilized tends to overestimate the triplet−singlet splitting of SO, for example, the splitting computed in test CCSD(T) calculations amounts to 23.8 kcal mol^{-1} versus an experimental value of 18.2 kcal mol^{-1} at 298 K.[23] This strongly suggests that also the spin allowed dissociation of $\mathbf{S_1}$ into SO_2 and SO ($a^1\Delta$) is energetically favored.

In conclusion, it appears that triplet $\mathbf{T_1}$ is the best theoretical description of the experimentally observed S_2O_3 molecule to be regarded as a metastable species. In this connection, the theoretical results are not inconsistent with the experimental detection of S_2O_3 as an isolated molecule with a lifetime >1 μs. Indeed the barrier to dissociation of $\mathbf{T_1}$, 6.1 kcal mol^{-1} at 298 K, is slightly lower than generally regarded as necessary to survive the neutralization event, although detection of species whose barrier to dissociation is as low as 6 kcal mol^{-1} is not unprecedented in NR experiments.[24] Furthermore, the barrier height computed at the CCSD(T) level is to be regarded as approximate, since the accurate theoretical analysis of the S_2O_3 system would require a complete multireferenced treatment.[25]

In any case, this study reports the first experimental detection of the hitherto unknown S_2O_3 oxide. Indeed, a blue-greenish solid prepared by dissolution of sulfur into SO_3 was long considered a polymeric sulfur oxide ("sulfur hemitrioxide") containing S−S bonds.[26] More recently, the solid was characterized as a salt of the S_4^{2+} cation and a polysulfate anion and its color traced to contamination by $S_3^{\bullet+}$.[27] The instability of S_2O_3 underlined by the present results accounts for the previous failure to detect this simple member of the large family of sulfur oxides, pointing again to the unique ability of NR techniques to prepare exotic or unstable species, inaccessible by conventional approaches.

Atmospheric Implications. The inventory of $S_2O_3^+$ ions in Io's atmosphere depends on the rate of reaction 2, affected in turn by two factors: (i) the supply of the SO^+ precursor and (ii) the SO_2 density in the regions where the reaction takes place. Indeed, a sufficient SO_2 density is required to allow significant collisional stabilization of the $S_2O_3^+$ ions from reaction 2, preventing their complete back dissociation observed in the low-pressure range (10^{-8} to 10^{-7} Torr) of the FT-ICR experiments. As to the first factor, whereas the average atmospheric ion density is low,[28] intense ion beams from the exosphere, where

(22) (a) Holmes, J. L. *Mass Spectrom. Rev.* **1989**, *8*, 513 and references therein. In this connection, no detailed calculations were performed concerning neutral S_2O_3 species of different connectivity, e.g. those from the neutralization of the thiosulfate anion, containing a S−S and theoretically examined by: (b) McKee, M. L: *J. Am. Chem. Soc.* **1993**, *115*, 9136.

(23) Huber, K. P.; Herzberg, G. *Constants of Diatomic Molecules*, Van Nostrand: New York, 1978.

(24) Schröder, D.; Schalley, C. A.; Goldberg, N.; Krůsák, J.; Schwarz, H. *Chem. Eur. J.* **1996**, *2*, 1235 and references therein.

(25) Kellog, C. B.; Schaefer, A. F. *Theor. Chem. Acc.* **1997**, *96*, 7.

(26) Weber, R. *Berichte* **1886**, *19*, 86.

(27) (a) Schenk, P. V.; Steudel, R. In *Inorganic Sulphur Chemistry*; Nickless, G., Ed.; Elsevier: Amsterdam, 1968; Chapter 11. (b) King, R. B.; *Encyclopedia of Inorganic Chemistry*; Wiley: New York, 1994; Vol. 7, p 3962 and references therein.

(28) The average ion density in the atmosphere is of the order of 10^3 cm^{-3}, personal communication of J. Moses.

SO^+ is a major species, are believed to impinge on the lower atmosphere and even on the frost SO_2 surface, causing its heating and sublimation, according to the "sputtering" atmosphere model.[29] As to the second factor, the most recent models point to the patchy structure of the Io atmosphere, formed by thin and thick regions with SO_2 columnar densities up to 3×10^{17} and 10^{19} cm^{-2}, respectively.[30] It appears that in the thick patches, covering some 35% of Io's disk, partial stabilizion of the $S_2O_3^+$ from reaction 2, and hence its presence in that atmosphere, are very likely. In this connection, the properties of the ion computed in this study may prove useful to its actual detection by optical or ion cyclotron spectrometry in future observational studies. The role of S_2O_3 is much more uncertain. It could be formed in the gas phase by charge exchange, for example with SO, or more likely following adsorption onto the frozen SO_2 surface. In this connection, we note that analysis of UV images of Io's surface taken with the Hubble space telescope has revealed the presence of sulfur oxides other than SO_2.[31]

Acknowledgment. This work was supported by the University of Rome "La Sapienza", the University of Perugia, the Ministero dell'Università e della Ricerca Scientifica e Tecnologica (MURST), and the Consiglio Nazionale delle Ricerche (CNR). We thank F. Angelelli and A. Di Marzio for their invaluable help.

JA002533D

(29) Sieveka, E. M.; Johnson, R. E. *J. Geophys. Res.* **1985**, *90*, 5327. (b) Pospieszalka, M. K.; Johnson, R. E. *Geophys. Res. Lett.* **1992**, *19*, 949.

(30) Hendrix, A. R.; Barth, C. A.; Hord, C. W. *J. Geophys. Res.* **1999**, *104*, 11817 and references therein.

(31) Clarke, J. T.; Ajello, J.; Luhmann, J.; Schneider, N.; Kanik, I. *J. Geophys. Res.* **1994**, *99*, 8387,